Finite Element Modeling and Simulation of Shaft Torsion Resistance and Teaching Application in Vocational Colleges

Meiqin Liang[1], Shang Wang[2*] and Xiaozhan Li[3]

[1]*College of Automation Engineering, Beijing Polytechnic, Beijing 100176, China*
[2]*School of Automotive Engineering, Beijing Polytechnic, Beijing 100176, China*
[3]*Institute of Engineering Technology, University of Science and Technology Beijing, Beijing 100086, China*
**Corresponding author: wangshang@bpi.edu.cn*

Abstract

Many knowledge points of Material Mechanics are abstract and difficult to understand for students in vocational colleges. In practical teaching, some students questioned the torsional resistance formula of hollow shaft. In order to solve students' learning doubts, this paper proposes a solution using modeling and simulation. The students and the teachers divided the work. Geometric model modeling and data analysis are completed by the students, while finite element modeling and simulation calculation are completed by the teachers. The Mises stress nephograms obtained by simulation calculation provide data to support the students' understanding, and completely solved the students' doubts. In addition, the students' analysis ability and data processing ability have been improved and exercised in the process of problem solving. Finite element modeling and simulation can provide a good solution to the doubts of students in vocational colleges, which is worth exploring by more scholars.

Keywords: *simulation, modeling, finite element simulation, shaft torsion resistance, vocational education.*

1.INTRODUCTION

Vocational education is an important part of the national education system. In recent decades, vocational education has provided strong talent support for the rapid development of the national economy. With the acceleration of industrial upgrading and economic transformation, the demand for high-level skilled talents in various industries is increasing, and the importance of vocational education is becoming more and more prominent [1][6]. In order to cope with the industrial upgrading and cultivate more excellent skilled applied talents for enterprises, the curriculum system of vocational colleges in various countries is also constantly exploring and reforming [4].

Material Mechanics is an important basic course in vocational colleges. Its content is the basis of other related professional courses, such as Mechanical Design Principle, Mechanical Manufacturing Engineering and Material Processing Engineering [13]. At present, the content of Material Mechanics courses in vocational colleges is based on ordinary undergraduate colleges, which lacks the characteristics of vocational education. As is known to all, students in vocational colleges have weak learning ability and understanding ability. Many formulas of Material Mechanics need complex mathematical derivation processes, and students generally feel great academic pressure and have no interest in learning [3].

Experimental teaching is an important way to further study and consolidate classroom content. In addition, experimental teaching can also stimulate students' interest in learning and exercise students' practical ability. However, the problem of poor teaching quality of Material Mechanics experiment course in vocational colleges has existed for a long time [11]. For instance, the equipment in many mechanics laboratories is old and small, which is difficult to meet the teaching needs. Many vocational colleges have only one experimental equipment. Only one teacher operated and dozens of students observed around the experimental equipment. Therefore, only three or four students in the front row can see the whole experimental process clearly. Figure 1 shows the torsion experiment of the shaft. If a class of 40 people only uses this equipment for experimental teaching, the teaching quality must be very poor.

A. El-Hashash et al. (Eds.): IEIT 2022, ACSR 100, pp. 206–214, 2023.
https://doi.org/10.2991/978-94-6463-058-9_36

Although the school has a lot of equipment, many times the experimental teacher only uses one for safety reasons [9]. During the experiment, the sample will be distorted. It is difficult for students to see the experimental phenomenon clearly, let alone understand the stress distribution of the sample, as shown in Figure 1. The problem of poor teaching quality of torsion resistance experiment has existed for a long time. However, the teaching of torsion resistance experiment is very important. On the one hand, the concept of torsional resistance is more abstract, which is difficult for students to understand. On the other hand, the torsion resistance experiment of shaft is often used in many jobs, such as the design of automobile transmission shaft and various reduction gearbox. As one of the basic experiments to test the properties of materials, the experimental teaching of torsional resistance mechanics in vocational colleges should be paid attention to.

Figure 1: Experimental equipment for shaft torsional resistance. (photo credit: original)

With the improvement in computing ability of computers and the popularization of simulation software, simulation technology has been greatly developed in many fields, such as metallurgy [7][12], transportation [2], medical treatment [5][8], military and education [10]. However, there is little research on modeling and simulation of torsion resistance experiment. In order to improve the teaching quality and solve the students' learning doubts, the research team carried out the finite element modeling of bending resistance experiment. The stress nephograms and data obtained from the simulation effectively solved the students' doubts. The simulation material has also been used in teaching and achieved good teaching results. The main research work of this paper includes:

(1) In the class of Materials Mechanics, some students raised the question about shaft torsion resistance. The students hoped to do relevant experiments and combine the experimental results to verify their views.

(2) The school has no relevant experimental equipment, so the experimental needs of students cannot be met. In order to actively the students' learning doubts, the research team proposed the solution of finite element modeling and simulation.

(3) The students and teachers divided the work. The students were responsible for the geometric model and the data processing, while the teachers were responsible for the finite element modeling and simulation.

(4) A finite element model consisting of two sub-models was established by ABAQUS.

(5) The two sub-models under different external loads were calculated separately, and the animations and the Mises stress nephograms were obtained.

(6) These simulation materials solved the students' doubts. In the process of solving problems, many abilities of students have been exercised and improved.

The research logic of this paper is shown in Figure 2.

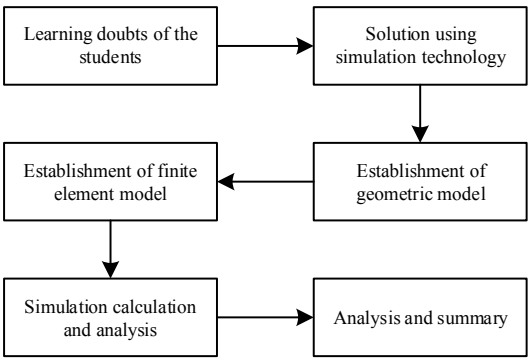

Figure 2: The research logic diagram of the paper. (figure credit: original)

2.PROBLEMS AND SOLUTIONS

After learning the knowledge of shaft chapter, some students do not have a deep understanding of torsional resistance. Some students mistakenly believe that solid shafts have better torsional resistance.

2.1. Problems

According to the textbook of Material Mechanics, the hollow shafts have better torsional resistance than the solid shafts when the cross-sectional area of both is equal.

Some students believe that the regions of solid shaft are closely connected. Compared with hollow shaft, solid shaft can transfer force better between various areas. Therefore, solid shafts perform better in torsional resistance.

The students' views conflict with the content of the textbook of Material Mechanics. There are clear conclusions in the textbook: the torsion resistance of hollow shaft is stronger. The research team explained to the students, but they still had doubts. The students hope to do mechanical experiments to verify their doubts. Unfortunately, the school has no relevant equipment, so the experimental needs of the students cannot be met.

2.2. Solutions

In order to solve the students' doubts and enhance their interest in learning, the research team proposed a solution using finite element modeling and simulation calculation.

The teachers and the students divided the work. The students are mainly responsible for two tasks. One is the establishment of geometric model, which needs to determine the specific size. The second is the later data processing obtained from the simulation, which needs to use the corresponding coordinate images of the software.

The teachers are mainly responsible for finite element modeling and simulation calculation. The teachers briefly introduced the basic theory and software operation of finite element to the students.

3.MODELING

Before establishing the finite element model, it is necessary to determine the geometric size of the model and the specific simulation requirements (test requirements). This part of the work is completed by the students under the guidance of the teachers.

3.1. Geometric Model

In order to determine the geometric model, the students carefully read the Material Mechanics textbook and consulted a lot of materials on the Internet.

The final geometric models are determined, as shown in Figure 3 and Figure 4. Model A is a solid shaft, with length of L=500 mm and diameter of d_1=60 mm, as shown in Figure 3.

Model B is a hollow shaft with a length of L=500 mm, which is equal to the solid shaft. The outer diameter of the hollow shaft is d_2=100 mm and the inner diameter is d_3=80 mm, as shown in Figure 4.

The parameters and requirements of the simulation are determined by the students. The simulation parameters are as follows:

One end of the shaft is fixed, and the other end is twisted by a fixed angle under the action of force coupling. The angles are set as 0.5°~3°, and the step factor is 0.5.

The data to be simulated are as follows:

(1) The stress/strain distributions of the two shafts under different torsion angles should be obtained.

(2) Maximum Mises stress of the two models corresponding to different torsion angles should be obtained.

(3) Torsional moment values corresponding to different torsion angles should be obtained.

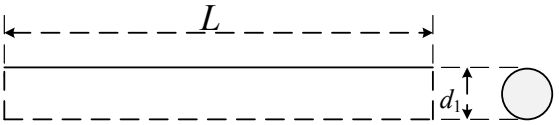

Figure 3: Geometric model of the solid shaft (Model A). (figure credit: original)

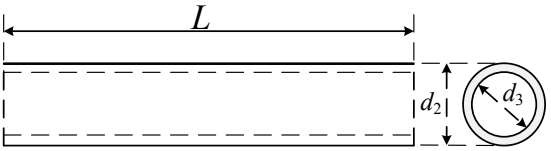

Figure 4: Geometric model of the hollow shaft (Model B). (figure credit: original)

3.2. Finite Element Model

According to the students' geometric models parameters, the finite element model is established. The finite element model includes two sub models (Model A and Model B). In order to facilitate the application of loads and constraints, a fixed base and a device for torsion are added on the basis of the original geometric model, as shown in Figure 5.

The geometric dimension of Model A is completely consistent with Figure 3. The length and width of the base of the model are 200 mm and the height is 20 mm. The torsion device of the model is a round cake with a diameter of 120 mm and a thickness of 10 mm. There are two handles on the round cake to facilitate loading.

Both shafts are made of steel. Setting of material property of the two models:

(1) Density of the material ρ=7.9×10^3 kg/m^3.

(2) Elastic modulus E=210 GPa, and Poisson's ratio λ=0.3.

(3) Three sets of data are set for plastic deformation, which are as follows: σ_1=418 MPa, ε_1=0; σ_2=500 MPa, ε_2=0.0158; σ_3=606 MPa, ε_3=0.0298; σ_4=829 MPa, ε_4=0.25; σ_5=932 MPa, ε_5=0.55; σ_6=1040 MPa, ε_6=0.85.

Two special points are defined and bound to two rigid bodies in the models. In order to set "Load" and "Boundary condition" more reasonably, operation points RP-1 (0, 0, -20) and RP-2 (0, 0, 550) are created in each sub-model. The fixed base is set as a "Rigid body" and bound to the point RP-1, while the device for applying torsion is set as a "Rigid body" and bound to the point RP-2.

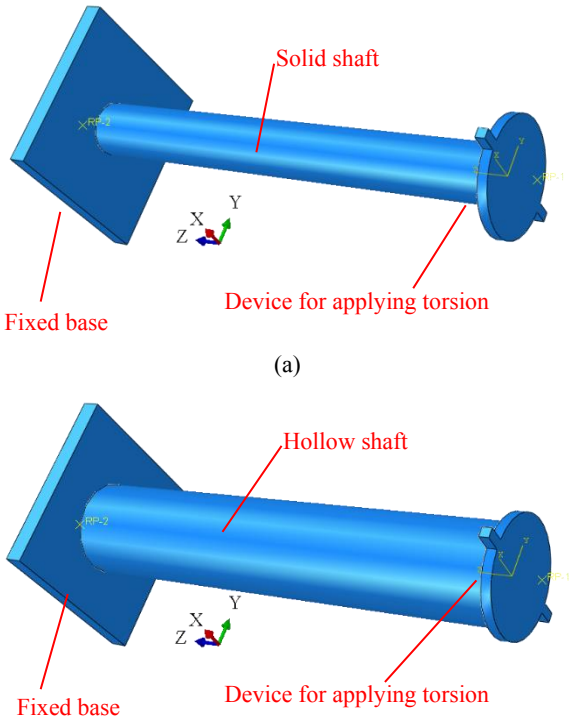

Figure 5: Finite element models and the coordinate system: (a) solid shaft; (b) hollow shaft. (figure credit: original)

The "Tie" command is used to connect parts in ABAQUS. One end of the solid shaft is connected with the base through the "Tie" command. Similarly, the other end is connected with the device for applying torsion through the "Tie" command. The setting of hollow shaft is exactly the same as that of solid shaft.

In the ABAQUS software, "Element type" of each shafts are selected as C3D10, while the fixed base and applying torsion device are selected as C3D8R.

The two shafts have the type "Tet" selected in the "Element shape" command, and in the "Global seeds" command the seeds size is set to 4 mm.

The fixed base in the two models has the type "Hex" selected in the "Element shape" command, and in the "Global seeds" command the seeds size is set to 10 mm. The applying torsion device in the two models has the type "Hex" selected in the "Element shape" command, and in the "Global seeds" command the seeds size is set to 5 mm. After the mesh is generated, the finite element model is shown in Figure 6.

In "Boundary condition" command, all six degrees of freedom of the RP-2 point are constrained, which means that the fixed base is completely fixed.

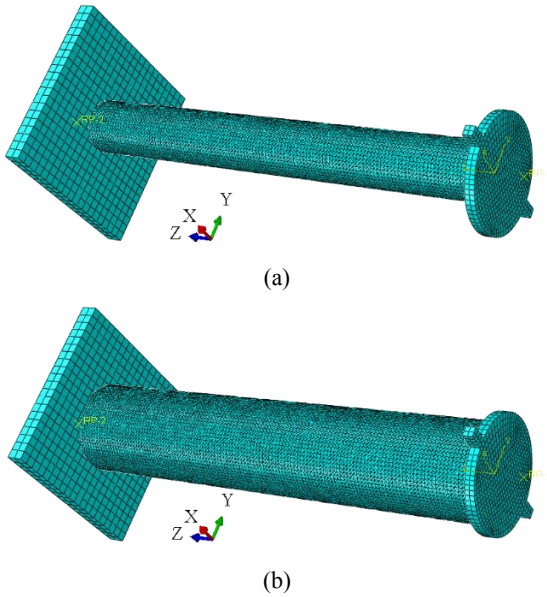

Figure 6: Finite element models after mesh generation: (a) solid shaft; (b) hollow shaft. (figure credit: original)

In "Load" command, the torsional force is applied to the RP-1 point. According to the test requirements of the students, the torsion angle of RP-1 point is applied. The parameters are set as follows: angles range 0.5°~3°, and the step factor is 0.5. In "Step" command, "statics-general" is selected, and the time of the "Step" is set to t=1 s. The "H-output" command is set to T=20 times.

4.SIMULATION CALCULATION AND ANALYSIS

According to the experimental needs of the students, loading was set up in the software. The finite element models were calculated on the computer. In all Mises stress nephograms, the applying torsion device is hidden to facilitate the observation of the cross section of the two shafts.

4.1. Simulation Results

When the applied torsion angle is 0.5 °, the calculated Mises stress nephograms of the finite element models are shown in Figure 7. Figure 7 (a) is a nephogram of Mises stress obtained after calculation by the Model A. Figure 7 (b) is a nephogram of Mises stress obtained after calculation by the Model B.

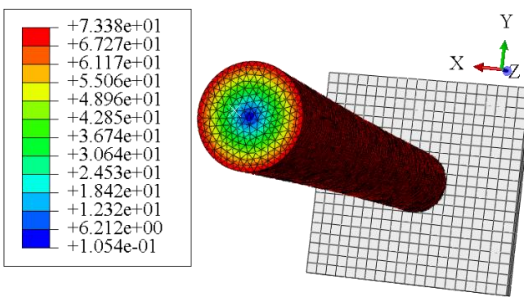

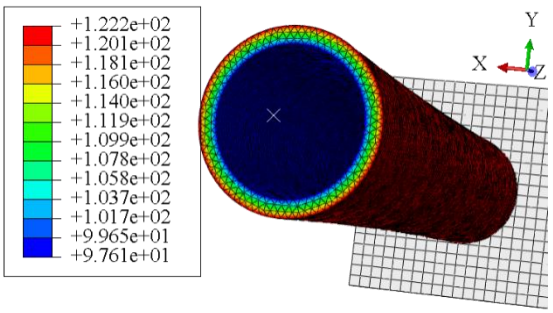

(b)

Figure 7: Mises stress nephograms of the finite element models with a 0.5° torsion angle: (a) Model A; (b) Model B. (figure credit: original)

As can be seen from Figure 7 (a), the stress distribution of the solid shaft is uneven, but the stress presents an axisymmetric law. The stress at the axis is small, while the stress on the shaft surface is large. This shows that when bearing the external torsion, the shaft bears a greater force near the surface, while the axial position bears a very small force. The maximum Mises stress in the model is 77.4 MPa (appearing on the shaft surface). As can be seen from Figure 7 (b), the stress distribution of the hollow shaft is also uneven, and the stress presents an axisymmetric law. The closer to the outer surface of the shaft, the greater the position stress. On the contrary, the closer to the inner surface of the shaft, the smaller the position stress. This shows that when the shaft is subjected to external torsion, it bears a greater force near the outside than the inner surface. The maximum Mises stress in the model is 122.2 MPa, which is much larger than that of the solid shaft. It can be seen from Figure 7 that the stress distribution of hollow shaft is relatively more uniform than that of solid shaft. The difference between the maximum stress and the minimum stress of the hollow shaft is 24.6 MPa, while the difference between the maximum stress and the minimum stress of the solid shaft is 73.3 MPa. This shows that when the same torsion angle occurs, each part of the hollow shaft bears a larger load, and its bending performance is excellent.

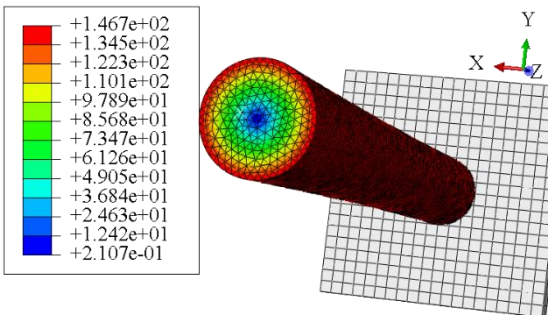

(a)

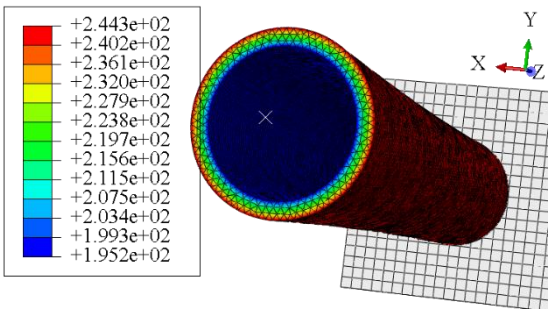

(b)

Figure 8: Mises stress nephograms of the finite element models with a 1° torsion angle: (a) Model A; (b) Model B. (figure credit: original)

Similarly, the finite element models conduct simulations on computers when the torsion angle is 1°. Mises stress nephograms of the finite element models are shown in Figure 8. Figure 8 (a) is a nephogram of Mises stress obtained after calculation by the Model A. Figure 8 (b) is a nephogram of Mises stress obtained after calculation by the Model B.

As can be seen from Figure 8 (a), the stress distribution of the solid shaft is uneven, but the stress presents an axisymmetric law, which is similar to Figure 7 (a). The stress at the axis is small, while the stress on the shaft surface is large. This shows that when bearing the external torsion, the shaft bears a greater force near the surface, while the axial position bears a very small force. The maximum Mises stress in the model is 146.7 MPa (appearing on the shaft surface). As can be seen from Figure 8 (b), the stress distribution of the hollow shaft is also uneven, and the stress presents an axisymmetric law. The closer to the outer surface of the shaft, the greater the position stress. On the contrary, the closer to the inner surface of the shaft, the smaller the position stress. This shows that when the shaft is subjected to external torsion, it bears a greater force near the outside than the inner surface. The maximum Mises stress in the model is 244.3 MPa, which is much larger than that of the solid shaft.

Figure 8 and Figure 7 show similar regularity: the stress distribution of hollow shaft is relatively more uniform than that of solid shaft. As can be seen from Figure 8, the difference between the maximum stress and the minimum stress of the hollow shaft is 49.1 MPa, while the difference between the maximum stress and the minimum stress of the solid shaft is 146.5 MPa. This shows that when the same torsion angle occurs, each part of the hollow shaft bears a larger load, and its bending performance is excellent.

When the torsion angle is 2°, the finite element models were calculated and the stress nephograms were obtained. Figure 9 (a) is a nephogram of Mises stress obtained after calculation by the Model A. Figure 9 (b) is a nephogram of Mises stress obtained after calculation by

the Model B. As can be seen from Figure 9 (a), the stress distribution of the solid shaft is uneven, but the stress presents an axisymmetric law. The stress at the axis is small, while the stress on the shaft surface is large. This shows that when bearing the external torsion, the shaft bears a greater force near the surface, while the axial position bears a very small force. The maximum Mises stress in the model is 293.5 MPa (appearing on the shaft surface). As can be seen from Figure 9 (b), the stress distribution of the hollow shaft is also uneven, and the stress presents an axisymmetric law. The closer to the outer surface of the shaft, the greater the position stress. On the contrary, the closer to the inner surface of the shaft, the smaller the position stress. This shows that when the shaft is subjected to external torsion, it bears a greater force near the outside than the inner surface. The maximum Mises stress in the model is 422.4 MPa, which is much larger than that of the solid shaft. According to the setting of the material properties of the model, the outer surface of the shaft has undergone plastic deformation. The metal flow caused by plastic deformation will inhibit the increase of Mises stress.

It can be seen from Figure 9 that the stress distribution of hollow shaft is relatively more uniform than that of solid shaft. The difference between the maximum stress and the minimum stress of the hollow shaft is 32.1 MPa, while the difference between the maximum stress and the minimum stress of the solid shaft is 293.1 MPa. This shows that when the same torsion angle occurs, each part of the hollow shaft bears a larger load, and its bending performance is excellent.

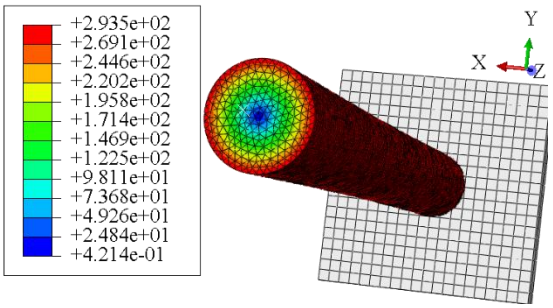

(a)

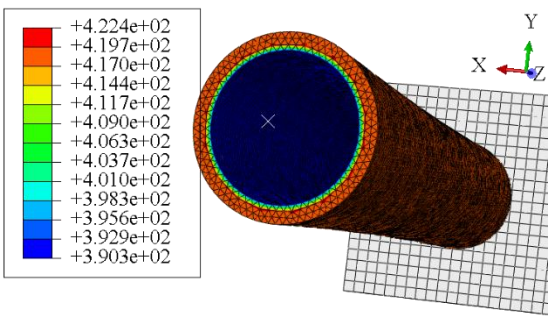

(b)

Figure 9: Mises stress nephograms of the finite element models with a 2° torsion angle: (a) Model A; (b) Model B. (figure credit: original)

When the torsion angle is 3°, the finite element models were calculated and the stress nephograms were obtained. Figure 10 (a) is a nephogram of Mises stress obtained after calculation by the Model A. Figure 10 (b) is a nephogram of Mises stress obtained after calculation by the Model B. As can be seen from Figure 10 (a), the stress distribution of the solid shaft is uneven, but the stress presents an axisymmetric law. The stress at the axis is small, while the stress on the shaft surface is large. This shows that when bearing the external torsion, the shaft bears a greater force near the surface, while the axial position bears a very small force. The maximum Mises stress in the model is 432.2 MPa (appearing on the shaft surface). As can be seen from Figure 10 (b), the stress distribution of the hollow shaft is also uneven, and the stress presents an axisymmetric law. The closer to the outer surface of the shaft, the greater the position stress. On the contrary, the closer to the inner surface of the shaft, the smaller the position stress. This shows that when the shaft is subjected to external torsion, it bears a greater force near the outside than the inner surface. The maximum Mises stress in the model is 424.9 MPa, which is much larger than that of the solid shaft.

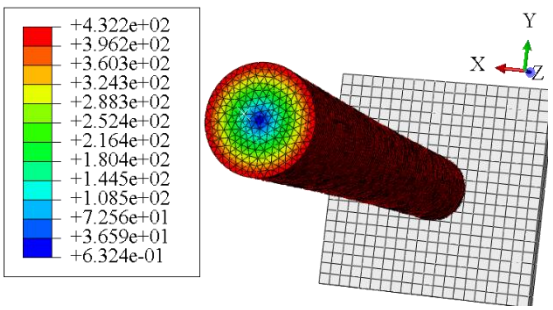

(a)

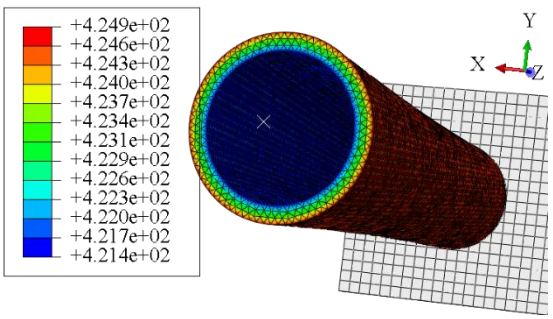

(b)

Figure 10: Mises stress nephograms of the finite element models with a 3° torsion angle: (a) Model A; (b) Model B. (figure credit: original)

Compared with Figure 9 (b), the maximum Mises stress does not change much. This is because the shaft surface has undergone plastic deformation at this time. Along the diameter direction of the shaft, the stress in the shaft is increasing. In Figure 10 (b), the minimum Mises stress (appearing on the inner surface) reaches 421.4 MPa, which is very close to the stress value of the surface. For comparison, the Mises stress on the shaft surface of a

solid shaft is 432.2 MPa, while the Mises stress at the shaft center is close to zero. This law also shows that when the same torsion angle occurs, each part of the hollow shaft bears a larger load, and its bending performance is excellent.

4.2. Statistics of Maximum Mises Stress and Applied Torsional Moment

In order to better compare the torsional resistance of solid shaft and hollow shaft, the maximum Mises stress and applied torque are statistically analyzed.

Figure 11 shows the statistics of the maximum Mises stress under different torsional angles. It can be seen from Figure 11 that the maximum Mises stress of the solid shaft is linear with the increase of the torsion angle. The maximum Mises stress of hollow shaft increases with the increase of torsion angle, which increases sharply in the initial stage and eases in the later stage. The maximum Mises stress increases slowly in the later stage because the shaft surface has undergone plastic deformation (as mentioned earlier).

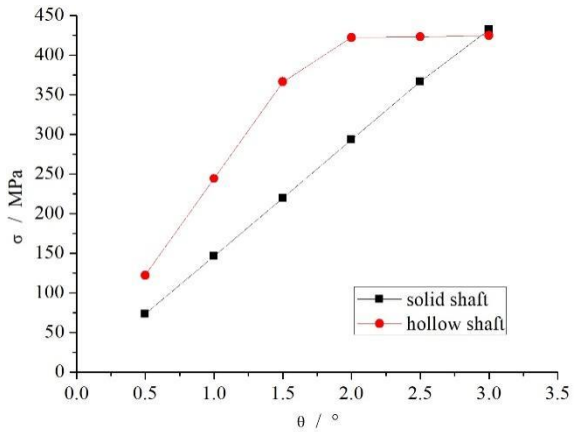

Figure 11: Statistics of maximum Mises stress under different torsional angles: (a) Model A; (b) Model B. (figure credit: original)

According to the comparative data, the maximum Mises stress of solid shaft is less than that of hollow shaft (except 3°) at the same torsion angle. This shows that the hollow shaft shows more obvious resistance when deflected at the same angle.

The statistical data of torsional moment also show a similar law. Figure 12 shows the statistics of torsional moment under different torsional angles. As can be seen from Figure 12, with the increase of torsional angle, the torsional moment of solid shaft increases. The two show a linear relationship. As can be seen from Fig. 12, the torsional moment of the hollow shaft increases with the increase of the torsional angle. The increase of initial torque value shows a linear relationship with a large slope. The increase of torque value in the later stage also shows a linear relationship, but the slope is small. The data in Figure 12 shows that the torque of hollow shaft is far greater than that of solid shaft. For example, when the torsion angle is 1°, the torque of the hollow bearing arm is 8.171 kN·m, while the torque of the solid bearing arm is only 1.794 kN·m. The former is 4.55 times that of the latter. This is enough that the torsion resistance of the surface hollow shaft is much better than that of the solid shaft. Similarly, when the torsion angle is 2°, the torque of the hollow bearing arm is 30.64 kN·m, while the torque of the solid bearing arm is only 7.137 kN·m. The former is 4.29 times that of the latter.

In short, the above Mises stress nephograms and data statistical chart have solved the students' doubts. The students have a deeper understanding of the torsional performance of hollow shaft. These materials have also been applied by the research team and classroom teaching, and achieved good teaching results.

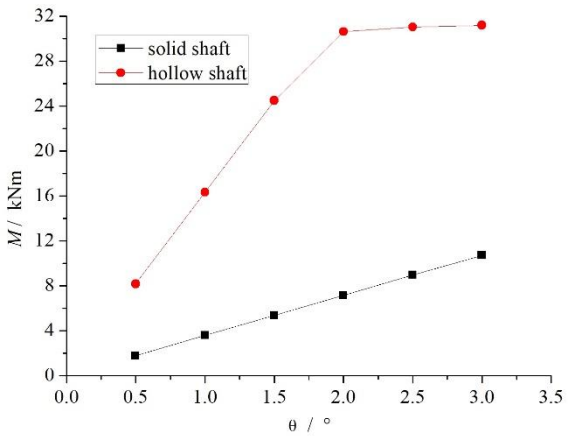

Figure 12: Statistics of applied torsional moment under different torsional angles: (a) Model A; (b) Model B. (figure credit: original)

5.RESULTS

Students in vocational colleges are poor in learning and understanding. Torsion is an important and difficult point in Material Mechanics. Many concepts of torsion, are dull, abstract and involve complex mathematical reasoning, which leads to a lack of interest among students. Pictures, animations and other materials that can intuitively show shaft stress/strain are urgently needed for the students of vocational colleges.

As mentioned above, with the joint efforts of the students and the teachers, the finite element model was established by ABAQUS. The finite element model was calculated on a computer, and thereby a large number of pictures, animations and data were obtained.

Abundant data and stress nephograms solved the students' doubts. The students participated in the whole process of solving problems, and their abilities in many aspects have been exercised. The students completed the following work:

J1: Consult the data to determine the specific size of the sample.

J2: Determining specific needs for test data.

J3: Making a three-dimensional drawing of the sample. After completing J3, the students' drawing ability has been improved.

J4: Processing the data, wherein Figure 11 and Figure 12 are all drawn by the students using the "Origin" software based on the simulation data.

J5: Writing a test report. Similar to J4, the students completed project reports under the guidance of the teachers. The report contains figures, tables and formulas. The process of systematically writing out reports is not only the process of consolidating the students' knowledge, but also the process of the growth of their analytical ability.

The questionnaire was carried out and the survey questions are as follows:

Q1: Does the simulation solve your problem?

Q2: Has your problem analysis ability been improved?

Q3: Has your data analysis ability been improved?

Q4: Has your drawing ability been improved?

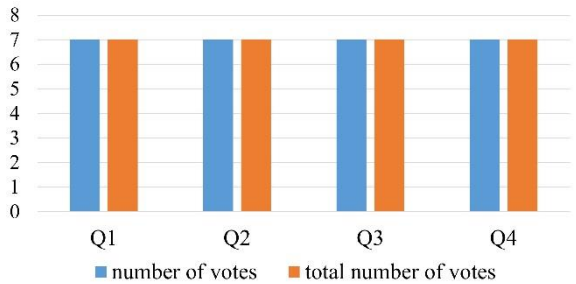

Figure 13: A questionnaire about ability improvement. (figure credit: original)

The statistical data is shown in Figure 13. All the students answered "yes" to the above questions. In view of the improvement of personal ability, the research team communicated with the students.

The students think their problem analysis ability has been improved. In the future work, they can deal with similar problems. In particular, they have mastered the idea of gradually overcoming problems. Similarly, the students have mastered the ability of data processing and can use "Origin" software to sort the data into a standard data graph.

In addition, the students' knowledge has been expanded. They learned about the basic theory of finite element and the basic principles of ABAQUS software. In particular, two students are interested in simulation technology and ABAQUS software. They said they would take time to learn the software. Students are interested in learning and willing to take the initiative to learn, which is what all teachers want to see. From this point of view alone, the efforts of the research team are valuable.

In short, the students' doubts were solved. In the process of solving problems, the students' various abilities have been exercised and improved.

6.CONCLUSION

With the joint efforts of the students and the research team, the finite element model of torsional resistance is established and simulated on a computer. The simulated Mises stress nephograms solve the students' learning doubts. In the process of solving problems, the students' abilities have also been improved. The main conclusions of this paper are as follows:

(1) Finite element modeling and simulation technology can be used in the teaching reform of Material Mechanics. The simulated colored Mises stress nephograms are helpful for students to understand abstract concepts.

(2) It is very necessary to force students to participate in the problem-solving process. Students' ability of problem analysis and data processing can be significantly improved in the process of participation.

The application field of finite element modeling and simulation technology is very wide, and scholars in vocational colleges should pay attention to it.

ACKNOWLEDGEMENTS

The research of this paper is supported by the Project of Beijing Office for Education Sciences Planning (Grant No. CCDB2020135 and No. CGDB21208), and by the Project of China Vocational Education Association (Grant No. ZJS2022YB024).

REFERENCES

[1] Chen Y. (2014). Teaching reform and practice on course of mechanics of materials. J. Journal of Jianghan University (Natural Science Edition), 42(04):40-44.

[2] Kastratović G, Vidanović N. (2015). 3D finite element modeling of sling wire rope in lifting and transport processes. J. Transport, 30(2): 129-134.

[3] Liu J. (2012). Exploration on teaching reform and innovation of material mechanics[C]//Advanced Materials Research. Trans Tech Publications Ltd, 591: 2208-2211.

[4] Rosina H, Virgantina V, Ayyash Y, et al. (2021). Vocational education curriculum: Between vocational education and industrial needs. J. ASEAN Journal of Science and Engineering Education, 1(2): 105-110.

[5] Scalese R J, Obeso V T, Issenberg S B. (2008). Simulation technology for skills training and

competency assessment in medical education. J. Journal of general internal medicine, 23(1): 46-49.

[6] Shi W. (2013). Issues and problems in the current development of vocational education in China. J. Chinese Education & Society, 46(4): 12-21.

[7] Solonenko O P, Kudinov V V, Smirnov A V, et al. (2005). Micro-metallurgy of splats: theory, computer simulation and experiment. J. JSME International Journal Series B Fluids and Thermal Engineering, 48(3): 366-380.

[8] Spooner N, Hurst S, Khadra M. (2012). Medical simulation technology: educational overview, industry leaders, and what's missing. J. Hospital topics, 90(3): 57-64.

[9] Wang S. (2022). Teaching research of material mechanics aimed at stimulating vocational college students' interest based on simulation technology. J. Scientific and Social Research, 4(3): 77-83.

[10] Wang S, Wang X, Feng Z, et al. (2021). Exploration on teaching of material mechanics in higher vocational colleges based on expansion of finite element theory[C]//2021 2nd International Conference on Information Science and Education (ICISE-IE). IEEE, 2021: 1535-1539.

[11] Wang T, Luo H F, Wang J, et al. (2016). Exploration and practice of material mechanics teaching reform. J. Experimental Science and Technology, 14(3): 116-118.

[12] Xu T, Song G, Yang Y, et al. (2021). Visualization and simulation of steel metallurgy processes. J. International Journal of Minerals, Metallurgy and Materials, 28(8): 1387-1396.

[13] Zhang J W, Zhu M J, Zhang L W. (2011). Teaching research and practice on material mechanics with the core of practical cases. J. Procedia Engineering, 15: 4256-4260.